

Cite this: *Soft Matter*, 2012, **8**, 5309

www.rsc.org/softmatter

PAPER

Facile preparation of coating fluorescent hollow mesoporous silica nanoparticles with pH-sensitive amphiphilic diblock copolymer for controlled drug release and cell imaging†

Xiao Mei,^a Dongyun Chen,^a Najun Li,^{*a} Qingfeng Xu,^a Jianfeng Ge,^a Hua Li,^a Baixia Yang,^b Yujie Xu^{*b} and Jianmei Lu^{*a}

Received 8th December 2011, Accepted 14th February 2012

DOI: 10.1039/c2sm07320j

A smart fluorescent drug carrier based on hollow mesoporous silica (HMS) nanoparticles was prepared step by step. First, HMS nanoparticles were doped with lanthanide rare-earth nanocrystals (YVO₄:Eu³⁺). Then the surface of HMS@YVO₄:Eu³⁺ was modified by octadecyltrimethoxysilane (C18). Afterwards, it was coated by designed pH-sensitive amphiphilic diblock copolymer (poly(MPEG-*b*-DBAM), PMD) through hydrophobic van der Waals interactions. The results of characterization such as transmission electron microscopy (TEM) and Fourier transform infrared spectroscopy (FT-IR) reveal that the material shows excellent monodisperse spherical morphology and narrow size distribution (180 nm) with hollow-core@mesoporous-silica-shell@thin-polymer-film structure. The multifunctional system HMS@YVO₄:Eu³⁺@C18@PMD was utilized to deliver the model drug ibuprofen (IBU), and the drug loading content of the system is as high as 834 mg/g (drug/carrier). Due to the coated pH-sensitive polymer film, the loaded drug is selectively released in mildly acidic environment. The time of release of about 80% drug was however prolonged from 50 to 150 h (at pH = 5.0) by the effect of modified C18, which has thus achieved longer-term release. Besides, the prepared material is easily imported into human mouth epidermal carcinoma (KB) cells and showed good and stable red fluorescence, which is suitable for cell imaging.

Introduction

Today, thousands of anti-cancer drugs such as doxorubicin (DOX), paclitaxel (PTX) and hydroxycamptothecin (HCPT)^{1–4} have been applied in clinical treatment. However, common anti-cancer drugs are water-insoluble, and display toxicity and side effects towards normal cells. Hence, many researchers pay great attention to “drug delivery”, and a variety of materials such as inorganic nanoparticles,^{5–8} polymeric nanoparticles,^{9–11} liposomes,¹² dendrimers,^{13,14} and others¹⁵ have been designed as smart materials which are able to deliver anti-cancer drugs to targeted sites in a controlled manner. Among the drug delivery materials mentioned above, the family of mesoporous silica nanoparticles (MSNs), such as MCM-*n*,^{16,17} SBA-*n*,^{18,19} CMS²⁰

and HMS,^{21–26} are generally considered as ideal drug delivery candidates due to their high level of biocompatibility and adjustable morphologies, effective property to deliver anticancer drug into tumors and excellent tumor suppressing effect,²⁷ and modifiable outer surface with abundant Si–OH.

To achieve controlled drug release, MSNs are often designed to be coated by other functional materials, such as functional nanoparticles,^{6,28–30} supramolecular nanovalves^{31,32} and biomacromolecular caps,^{33–35} especially coating of MSNs with functional polymers.^{36–38} Due to its broad applicability in drug delivery, gene delivery and other biomedical applications, polymer-coated systems have been extensively studied. Many methods including free radical polymerization, reversible addition–fragmentation chain transfer (RAFT), emulsion polymerization, and solid-oil-in water (S/O/W) emulsification have been developed. For example, Gao and co-workers coated several layers of poly-methylacrylic acid-co-vinyl triethoxysilane (PMV) onto mesoporous silica by the free radical polymerisation method, and this material showed pH responsive release of ibuprofen.³⁶ Lin and co-workers coated thermosensitive poly-*N*-isopropylacrylamide (PNIPAm) onto the outer surface of MSNs via RAFT and this composite can be utilized to prepare nanovalves based on thermally responsive MSN, where drugs can be released at a certain temperature.³⁹ However, in such systems, the

^aLaboratory of Absorbent Materials and Techniques for Environment, College of Chemistry, Chemical Engineering and Materials Science, Soochow University, Suzhou, China 215123. E-mail: lujm@suda.edu.cn; linajun@suda.edu.cn; Fax: +86 (0) 512-6588 0367; Tel: +86 (0)512-6588 0368

^bJiangsu Provincial Key Laboratory of Radiation Medicine and Protection, Medical College of Radiation Medicine and Protection, Soochow University, Suzhou, China, 215123. E-mail: dbnm@suda.edu.cn; Fax: +86 (0) 512-65884830; Tel: +86 (0) 512-6588 006

† Electronic supplementary information (ESI) available. See DOI: 10.1039/c2sm07320j

drug loading content is actually poor due to the blocking of the polymer in pore channels of MSNs when the drug was loaded after polymer was coated onto MSNs. Hence, it is crucial to develop a strategy that can offer the dual advantage of high drug loading content and effective functional polymer coating.⁴⁰

In this paper, we designed an easy method to solve the problem above (Scheme 1). We first chose HMS as support for a high drug loading content owing to its hollow core,^{22,23} then the surface of HMS was modified with long-chain hydrocarbon octadecyltrimethoxysilane (C18) moieties, and this strategy could have several advantages. First, it can modify the chemical interaction between the pore surface and the adsorbed drug, which can decrease the wettability of the surface by aqueous solutions and increase the amount of hydrophobic drug adsorption and further delay the drug release.⁴¹ Secondly, the modified alkyl chains are not able to close the pores but are suitable to interact with the pH stimuli-responsive amphiphilic diblock copolymer we designed through hydrophobic van der Waals interactions,^{42,43} so the HMS would be easily coated by functional polymer. The drug was loaded in HMS and then blocked by coated polymer. When specifically recognized and internalized by tumor cells, the coated pH-responsive polymer would hydrolyze into biocompatible polymer due to cleavage of acetal moieties in the weakly acidic endosomal/lysosomal compartments, resulting in encapsulated drug release. Furthermore, the surface of HMS was modified

with fluorescent material of lanthanide-doped rare-earth nanocrystals for cell imaging rather than organic dyes or quantum dots (QDs), due to their good optical properties, high chemical and photochemical stability and low toxicity.^{44–46} Hence, the polymer-coated system, prepared by an easy strategy, has potential applications of controlled drug release and cell imaging.

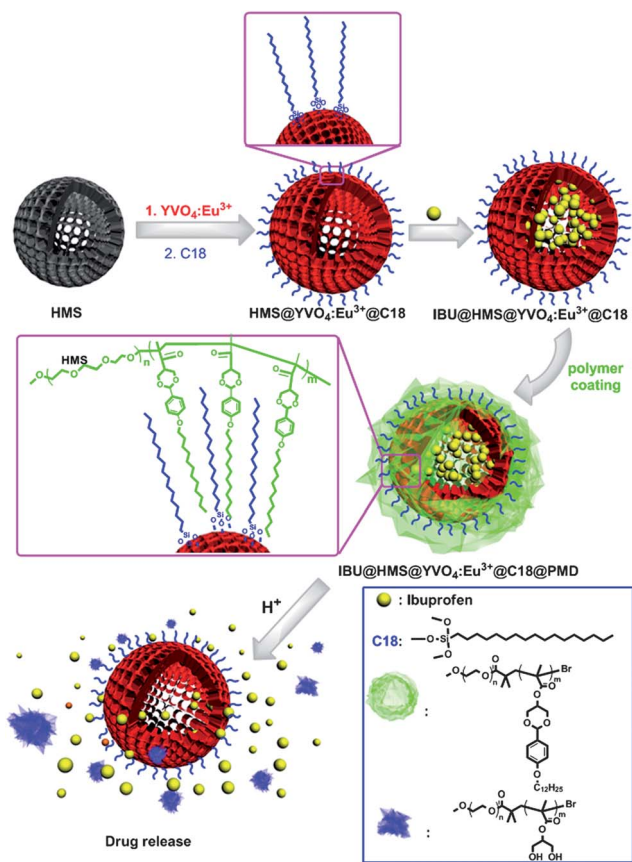
Experimental

Materials

(2-(Acryloyloxy)ethyl)trimethylammonium chloride (AETAC, 80 wt% in water), 2,2'-azobis(2-methylpropionamide) dihydrochloride (V-50, >97.0%), hexadecyltrimethylammonium bromide (CTAB, >99.0%) and octadecyltrimethoxysilane (C18) were purchased from Aldrich. Methoxy poly(ethylene glycol) (MPEG-OH, 5000 g mol⁻¹, Fluka) were dehydrated by azeotropic distillation of water in toluene, precipitated with cold ethyl ether, filtered, washed with diethyl ether and dried in vacuum. Tetraethoxysilane (TEOS), 2-bromoisobutyryl bromide, europium oxide (Eu₂O₃), yttrium(III) oxide (Y₂O₃) and ammonium vanadium oxide (NH₄VO₃) were purchased from Alfa without any purification. Styrene (St, >99.0%) was washed through an inhibitor remover column for removal of *tert*-butyl catechol and then distilled under reduced pressure prior to use. Tetrahydrofuran (THF) and cyclohexanone were purified by reduced pressure distillation. CuBr was purified until colorless by stirring in glacial acetic acid, consecutive washing with absolute ethanol and diethyl ether, and keeping under vacuum. Other reagents were commercially available and used as received.

Synthesis of hollow mesoporous spherical (HMS) particles

The hollow mesoporous spherical particles were synthesized according to the literature⁴⁷ with some modifications. To prepare the polystyrene latex templates, 1.0 g of AETAC (80 wt% in H₂O) was dissolved in 390.0 g water in a 500 mL round-bottom flask. 40.0 g styrene was added slowly to the solution and kept stirring at 800 rpm by mechanical raking for 30 min. The mixture was purged with nitrogen for 20 min and then heated to 90 °C with an oil-bath. Afterwards, 10 mL of an aqueous solution containing 1.0 g V-50 was added. The emulsion was kept at 90 °C for 24 h under nitrogen. The polystyrene latex was obtained by centrifugation at 1800 rpm for 15 min, and washed with ethanol several times. To obtain the HMS, 0.8 g of CTAB was dissolved in a mixture of 29.0 g of water, 12.0 g of ethanol and 1.0 ml of aqueous ammonia solution. 930 mg of PS powders was dispersed in 10.0 g water by sonication and then added dropwise to the above CTAB solution at room temperature under vigorous stirring, followed by sonication for 10 min. The derived milky mixture was then magnetically stirred for 30 min before adding dropwise 4.0 g of TEOS. The resulting mixture was kept stirring at room temperature for 48 h before the mesoporous silica coated latex was harvested by centrifugation at 7000 rpm for 40 min. The precipitate was washed with copious amounts of ethanol and then dried at room temperature. Finally the material was calcined in air at 600 °C for 8 h using a heating rate at 3 °C min⁻¹.



Scheme 1 Schematic depiction of the structure of IBU@HMS@YVO₄:Eu³⁺@PMD and controlled release by degradation under weakly acidic conditions.

Luminescence functionalization of HMS by $\text{YVO}_4\text{:Eu}^{3+}$ ($\text{HMS@YVO}_4\text{:Eu}^{3+}$)

Y_2O_3 (0.429 g, 1.9 mmol), Eu_2O_3 (0.0352 g, 0.1 mmol) and NH_4VO_3 (0.232 g, 2 mmol) were added into dilute HNO_3 (15 mL, 3 mol L^{-1}). After dissolving completely, the solution was added to a water–ethanol solution ($v/v = 1/7$), then citric acid (0.84 g, 4 mmol) and poly(ethylene glycol) (PEG, 10000 g/mol) was added. After stirring for 1 h, the solution turned into a blue homogenous sol, followed by adding 200 mg HMS and stirring for another 3 h. The product was separated by centrifugation, dried at 100 °C for 1 h, and calcined at 500 °C for 2 h. The obtained product was denoted as $\text{HMS@YVO}_4\text{:Eu}^{3+}$.

Modification of the external surface of $\text{HMS@YVO}_4\text{:Eu}^{3+}$ with octadecyltrimethoxysilane (C18) ($\text{HMS@YVO}_4\text{:Eu}^{3+}@C18$)

100 mg $\text{HMS@YVO}_4\text{:Eu}^{3+}$ was first dispersed in 20 mL anhydrous acetonitrile, then 5 mL C18 was added, and the obtained suspension was stirred for 24 h and collected by centrifugation, washed with acetonitrile and ethanol several times, and dried under vacuum. The obtained white solid was denoted as $\text{HMS@YVO}_4\text{:Eu}^{3+}@C18$.

Synthesis of 4-*n*-dodecyloxybenzal acetal monomer (DBAM)

p-Hydroxybenzaldehyde (5 g, 40.9 mmol) was dissolved in 150 mL acetone solution containing anhydrous potassium carbonate (16.8 g, 122 mmol), then 1-bromododecane (12.2 g, 49.2 mmol) was added slowly. After heating under reflux with stirring for 24 h, the acetone was evaporated. Then 100 mL water and 100 mL ethyl acetate were added. The organic layer was collected and washed with saturated NaCl solution twice and dried by anhydrous MgSO_4 overnight. After evaporating the ethyl acetate, the crude 4-*n*-dodecyloxybenzaldehyde (DBD) product was purified by column chromatography (ethyl acetate–petroleum ether, 1:5).

The obtained DBD (8.7 g, 30 mmol) was dissolved in 50 mL toluene with *p*-toluenesulfonic acid (PTSA) (0.5 g) as catalyst. Then glycerol (2.76 g, 30 mmol) was added and the mixture refluxed with vigorous stirring for 14 h, and the water by-product was removed by the oil–water separator. Then the mixture was evaporated and washed with potassium carbonate solution (1%, 80 mL) to remove the acid catalyst and any remaining glycerol. The crude product was purified by column chromatography (ethyl acetate–petroleum ether, 1 : 2), and a white product 4-*n*-dodecyloxybenzal acetal (DBA) was obtained.

To synthesize the final product DBAM, DBA (4.0 g, 11 mmol) and triethylamine (4.5 g, 44 mmol) were dissolved in anhydrous tetrahydrofuran (20 mL) and the mixture was cooled to 0 °C in an ice-bath. Then anhydrous tetrahydrofuran (5 mL) with methacryloyl chloride (2.3 g 22 mmol) was added slowly. After stirring at room temperature overnight, the mixture was filtered off and evaporated, and the crude product was purified by column chromatography (ethyl acetate–petroleum ether, 1 : 8). Anal. Calc. for $\text{C}_{26}\text{H}_{40}\text{O}_5$: C, 72.19, H, 9.32, O, 18.49. Found: C, 72.30, H, 9.28, O, 18.42%. ^1H NMR (400 MHz, CDCl_3), δ (ppm): 7.41 (d, $J = 8.39$ Hz, 2H, C_6H_4), 6.89 (d, $J = 8.41$ Hz, 2H, C_6H_4), 6.30 (s, 1H, CCH_2), 5.65 (s, 1H, CCH_2), 5.52 (s, 1H, $\text{C}_6\text{H}_4\text{CH}$), 4.75 (s, 1H, CHO), 4.31 (d, $J = 12.88$ Hz, 2H, CHCH_2O), 4.18 (d,

$J = 12.92$ Hz, 2H, CHCH_2O), 3.95 (t, $J = 6.59$ Hz, 2H, $\text{C}_6\text{H}_4\text{OCH}_2$), 2.01 (s, 3H, CH_3), 1.81–1.72 (m, 2H, $\text{CH}_2\text{CH}_2\text{O}$), 1.49–1.38 (m, 2H, $\text{CH}_2\text{CH}_2\text{CH}_2\text{O}$), 1.26 (m, 16H, CH_2), 0.88 (t, $J = 6.68$ Hz, 3H, CH_2CH_3). ^{13}C NMR (75 MHz, CDCl_3), δ 167.45 (s, 1C, COO), 159.95 (s, 1C, C), 136.28 (s, 1C, CCH_3), 132.25 (s, 1C, C), 127.57 (s, 2C, CH), 126.50 (s, 1C, CCH_2), 114.52 (s, 2C, CH), 74.21 (s, 1C, CH_2CO), 69.25 (s, 2C, CH_2CO), 68.28 (s, 1C, CHCH_2O), 32.16 (s, 1C, $\text{CH}_2\text{CH}_2\text{CH}_3$), 29.28–29.88, (m, 7C, CH_2), 26.24 (s, 1C, $\text{CH}_2\text{CH}_2\text{CH}_2\text{O}$), 22.94 (s, 1C, CH_2CH_3), 18.52 (s, 1C, CCH_3), 14.39 (s, 1C, CH_3).

Synthesis of diblock copolymer poly(MPEG-*b*-DBAM) (PMD)

The diblock copolymer MPEG-*b*-DBMA was synthesized by atom transfer radical polymerization (ATRP). First, the macroinitiator MPEG-Br was synthesized by reacting MPEG-OH with 2-bromoisobutryl bromide. A solution of MPEG-OH (5000, 10 g, 2 mmol) and triethylamine (400 mg, 4 mol) in anhydrous THF (35 mL) was slightly cooled in an ice–water bath. Then, a solution of 2-bromoisobutryl bromide (1.72 mL, 14 mmol) in anhydrous THF (5 mL) was slowly added to the reaction mixture. The solution was warmed to room temperature and stirred for 48 h. The mixture was poured into water (100 mL) and extracted with dichloromethane (5×20 mL). The organic extracts were washed successively with HCl (1 M), NaOH (1 M) and saturated NaCl solution, and dried by anhydrous MgSO_4 overnight. Then the solvent was removed under reduced pressure. The crude extract was dissolved in a minimum of dichloromethane and then precipitated in diethyl ether. The macroinitiator MPEG-Br was recovered by filtration.

To synthesize PMD, MAPEG-Br (2 g, 0.4 mmol) was added to a solution containing PMEDTA (76.25 mg, 0.44 mmol), CuBr (45.76 mg, 0.44 mmol), and DBAM (4.32 g, 10 mmol) in cyclohexanone (2 mL). The mixture was degassed with argon for 30 min at room temperature and then heated overnight at 90 °C. Then the mixture was diluted by 10 mL THF and filtered on neutral aluminum oxide gel, with THF as an eluent, to remove copper bromide. Finally, the product was concentrated and then precipitated in diethyl ether. The PMD was recovered by filtration.

Drug loading experiment ($\text{IBU@HMS@YVO}_4\text{:Eu}^{3+}@C18$)

Ibuprofen (IBU) was used as model drug according to the literature with some modifications.^{22,23} Ibuprofen (300 mg) was dissolved in hexane (5 mL), then, $\text{HMS@YVO}_4\text{:Eu}^{3+}@C18$ (100 mg) was added to this solution. After stirring for 24 h at room temperature, the $\text{HMS@YVO}_4\text{:Eu}^{3+}@C18$ with adsorbed IBU was separated by centrifugation and washed with a solution of pH 1.4 for several times. Finally, the product was dried at 60 °C in vacuum. This product is denoted as $\text{IBU@HMS@YVO}_4\text{:Eu}^{3+}@C18$.

To evaluate the amount of drug loaded by $\text{HMS@YVO}_4\text{:Eu}^{3+}@C18$, UV-Vis spectroscopy was used for analysis. First, the calibration curve of ibuprofen was determined by taking absorbance vs. ibuprofen concentration between 0 and 2 mg ml^{-1} as parameters, and the calibration curve was fitted to the Lambert–Beer law as follows:

$$A = 0.02584 + 0.99556C$$

where A is the absorbance and C is the concentration (mg ml^{-1}).

After adsorption, the IBU solution (0.1 mL) was extracted and diluted to 10 mL, and then analyzed by UV-Vis spectroscopy at a wavelength of 265 nm. The calculation of drug loading content is discussed below.

Synthesis of PMD-coated IBU@HMS@YVO₄:Eu³⁺@C18 (IBU@HMS@YVO₄:Eu³⁺@C18@PMD)

IBU@HMS@YVO₄:Eu³⁺@C18 (10 mg) and PMD (20 mg) were dissolved in tetrahydrofuran (1 mL). Then, 5 mL of distilled water was added to this solution with vigorous shaking. The mixture was kept stirring for 24 h at room temperature to evaporate tetrahydrofuran. After that, the product was separated by centrifugation and washed with distilled water several times to remove the unbound copolymer. The obtained product was denoted as IBU@HMS@YVO₄:Eu³⁺@C18@PMD.

In vitro experiments

In vitro drug-release study. The prepared IBU@HMS@YVO₄:Eu³⁺@C18@PMD sample (15 mg) was immersed in simulated body fluid (SBF) at 37 °C to maintain a constant temperature. The obtained colloid was divided into three equivalent parts and adjusted to different pH values by acetate buffer. The drug concentration was analyzed by UV-Vis spectroscopy.

Cell culture and preparation. Human mouth epidermal carcinoma (KB) cell line (purchased from Shanghai Cell Institute Country Cell Bank, China) were cultured as a monolayer in RPMI-1640 medium supplemented with 10% heat-inactivated fetal bovine serum at 37 °C in a humidified incubator (5% CO₂ in air, v/v).

In vitro cytotoxicity. The aminoxanthene dye, sulforhodamine B (SRB), was used as an assay for assessing the effects of drug carriers in various concentrations.⁴⁸ In brief, well-growing KB cells were placed in 96-well plates (1.3 × 10⁴ cells per well) and four duplicate wells were set up in the sample. The culture medium was replaced with the medium containing different concentrations of drug carriers (0, 0.390625, 0.78125, 1.5625, 3.125, 6.25, 12.5, 25, 50, 100 μg mL⁻¹) and cultured at 37 °C in a humidified incubator (5% CO₂ in air, v/v) with the cells anchored to the plates. After being cultured for 24 h, the medium was poured away and 10% (w/v) trichloroacetic acid in Hank's balanced salt solution (100 μL) was added and stored at 4 °C for 1 h. Then the stationary liquid was discarded, the cells were washed with deionized water five times before air drying and stained with 0.4% (w/v) SRB solution (100 μL per well) for 30 min at room temperature. After removing the SRB, the cells were washed with 0.1% acetic acid solution five times. Bound SRB dye was solubilized with 10 mmol L⁻¹ tris-base solution (150 μL, pH = 10.5). The optical density (OD) value of each individual well was calculated using a spectrophotometer at 531 nm absorbance.

Cellular uptake of HMS@YVO₄:Eu³⁺@C18@PMD. KB cells were seeded in 96-well plates (1.3 × 10⁴ cells per well) and incubated overnight at 37 °C in a humidified incubator. The dispersion of the HMS@YVO₄:Eu³⁺@C18@PMD sample was

prepared in RPMI-1640 medium. Cells were cultured with the HMS@YVO₄:Eu³⁺@C18@PMD solution for a certain time and observed using confocal laser fluorescence microscopy (Olympus, FV 1000) after washing three times with PBS.

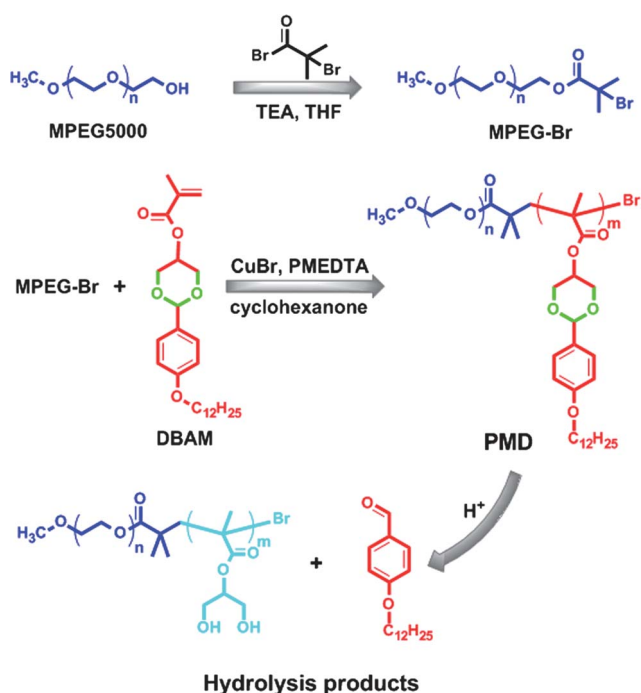
Characterization. FT-IR measurement was performed as KBr pellets on a Nicolet 4700 spectrometer (Thermo Fisher Scientific) in the range of 400–4000 cm⁻¹. Gel permeation chromatography (GPC) analysis was carried out on a Waters 1515 pump and a differential refractometer, THF was used as a mobile phase at a flow rate of 1.0 mL min⁻¹. ¹H and ¹³C NMR spectra were measured by an INOVA 400 MHz NMR instrument with CDCl₃ as deuterated solvent. Transmission electron microscopy (TEM) and high-resolution transmission electron microscopy (HRTEM) images were obtained by a TecnaiG220 electron microscope at an acceleration voltage of 200 kV. The sample for TEM and HRTEM observations was prepared by placing a drop of the dispersion of nanoparticles on copper grids. Energy dispersive spectrometry (EDS) was taken on a Hitachi S-4700 equipped with an energy-dispersive X-ray spectrum. Room-temperature emission and excitation spectra were carried out by using an Edinburgh-920 fluorescence spectrophotometer. Brunauer–Emmett–Teller (BET) and Barrett–Joyner–Halenda (BJH) analysis used to determine the surface area, pore size and pore volume were obtained with a Quantachrome Autosorb 1C apparatus at –196 °C under continuous adsorption conditions. The UV-Vis absorption spectra were measured on a TU-1901 spectrophotometer. Confocal laser scanning microscopy (CLSM) images were observed by confocal laser scanning microscope (Olympus, FV 1000).

Results and discussion

Synthesis and characterization of IBU@HMS@YVO₄:Eu³⁺@C18@PMD

Synthesis and characterization of diblock copolymer PMD. The synthetic process of PMD is shown in Scheme 2. Three diblock copolymers with different *M_n* and PDI were synthesized by varying the mole ratio of the macroinitiator and the monomer. Based on an evaluation of the characterization data of the diblock copolymers, PMD polymerized with macroinitiator and the monomer feed ratio of 1 : 25 was chosen for further investigation (Table S1, ESI†). In addition, ¹H NMR of PMD clearly showed peaks corresponding to DBMA besides signals assignable to MPEG (Fig. S1, ESI†). These results signified that the structurally well-defined diblock copolymer PMD was successfully synthesized.

Synthesis and characterization of IBU@HMS@YVO₄:Eu³⁺@C18. The surface of HMS shell was first functionalized by the deposition of YVO₄:Eu³⁺ phosphor layer through a sol-gel process. From Fig. 1a we can see the noticeable difference between the hollow core and the mesoporous shell of HMS@YVO₄:Eu³⁺, which suggest that HMS@YVO₄:Eu³⁺ maintain well-defined hollow, mesoporous structures and keep the ability of loading drug. The clear lattice fringes deposited on the SiO₂ matrix in the HRTEM image (Fig. 1b) further confirm the high crystallization of the product. The average



Scheme 2 Schematic illustration of the synthetic route of PMD.

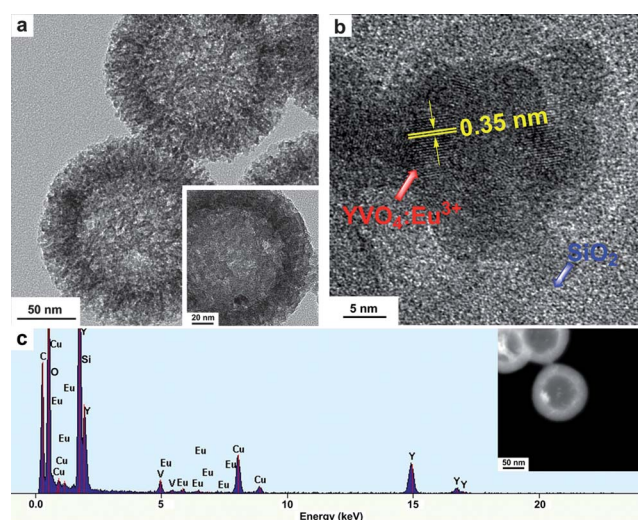


Fig. 1 TEM images (a), HRTEM (b) and EDX (c) (inset: acquire HAADF images) of HMS@YVO₄:Eu³⁺.

distances between adjacent lattice fringes are 0.35 nm, which are close to the d_{200} spacing (0.355 nm) of the tetragonal YVO₄ phase (JCPDS No. 17-0341). EDX (Fig. 1c) and EDS (Fig. S3, ESI[†]) spectra further confirmed the presence of silicon (Si), oxygen (O), yttrium (Y), and vanadium (V) in the HMS@YVO₄:Eu³⁺ sample. The signals of Cu and C in EDX are from the copper grid and carbon membrane for measurement. All of the results above reveal successful preparation of HMS@YVO₄:Eu³⁺ with a hollow core structure and mesoporous channels.

The FT-IR spectra of HMS@YVO₄:Eu³⁺, HMS@YVO₄:Eu³⁺@C18 and IBU@HMS@YVO₄:Eu³⁺@C18 are shown in Fig. 2. In the spectrum of HMS@YVO₄:Eu³⁺, the strong bands

of Si–OH (950 cm⁻¹) suggest a large number of silanol groups still exist on the surface of the rare earth-modified HMS, which play a key role for coupling alkyl chains. Besides, the band of OH (3429 cm⁻¹), Si–O–Si (1092 cm⁻¹) and H₂O (1635 cm⁻¹) are also present. After coupling C18, the new band of C–H_x (2890 cm⁻¹) clearly confirms the successful modification of C18. For IBU-loaded HMS@YVO₄:Eu³⁺@C18, the obvious new band at 1720 cm⁻¹ which is assigned to –COOH confirms the successful loading of IBU into HMS@YVO₄:Eu³⁺@C18.^{23,46} After coating the PMD, The absorption bands related with C=O (1740 cm⁻¹) and skeleton vibrations (1520 and 1620 cm⁻¹) of the benzene ring were observed, confirming that the polymer coated the HMS successfully.

Synthesis and characterization of IBU@HMS@YVO₄:Eu³⁺@C18@PMD. In our strategy, the prepared PMD would strongly associate with the hydrocarbon coupling agents C18 on the surface of HMS through hydrophobic van der Waals interactions owing to their large number of hydrophobic alkyl chains. The macroscopic state and microstructure of IBU@HMS@YVO₄:Eu³⁺@C18@PMD were evaluated by photographs and TEM, respectively. In visible light (Fig. 3a), the pure HMS has excellent dispersibility in water owing to the abundant silanol groups at the surface (Fig. 3a-1). After coupling C18, the nature of HMS was transformed into hydrophobic, which was easily dispersed in hexane and could no longer disperse in water well (Fig. 3a-2). The C18 plays a key role in the interaction between HMS and PMD, so IBU@HMS@YVO₄:Eu³⁺@C18 was easily coated by PMD *via* self-assembly. Finally, the prepared IBU@HMS@YVO₄:Eu³⁺@C18@PMD would restore hydrophilicity because of the hydrophilic segment in PMD (Fig. 3a-3). Under UV irradiation (Fig. 3b), no fluorescence was observed in an aqueous solution of pure HMS (Fig. 3b-1), while red fluorescence was evident for a hexane solution of IBU@HMS@YVO₄:Eu³⁺@C18 (Fig. 3b-2) and aqueous solution of IBU@HMS@YVO₄:Eu³⁺@C18@PMD (Fig. 3b-3), respectively. These results indicated IBU@HMS@YVO₄:Eu³⁺@C18@PMD with excellent water-solubility and good fluorescence was prepared.

To observe the microstructure, TEM images of IBU@HMS@YVO₄:Eu³⁺@C18@PMD (Fig. 3e–3f) were compared with

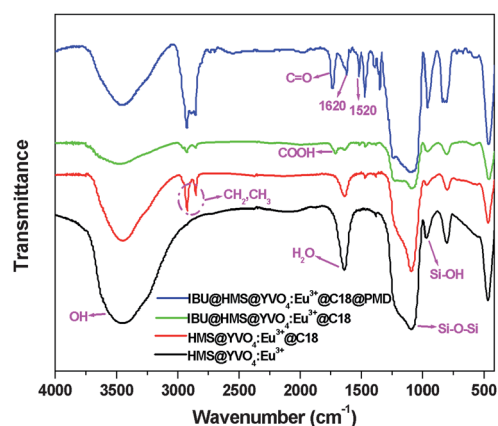


Fig. 2 FTIR spectra of HMS@YVO₄:Eu³⁺, HMS@YVO₄:Eu³⁺@C18 and IBU@HMS@YVO₄:Eu³⁺@C18.

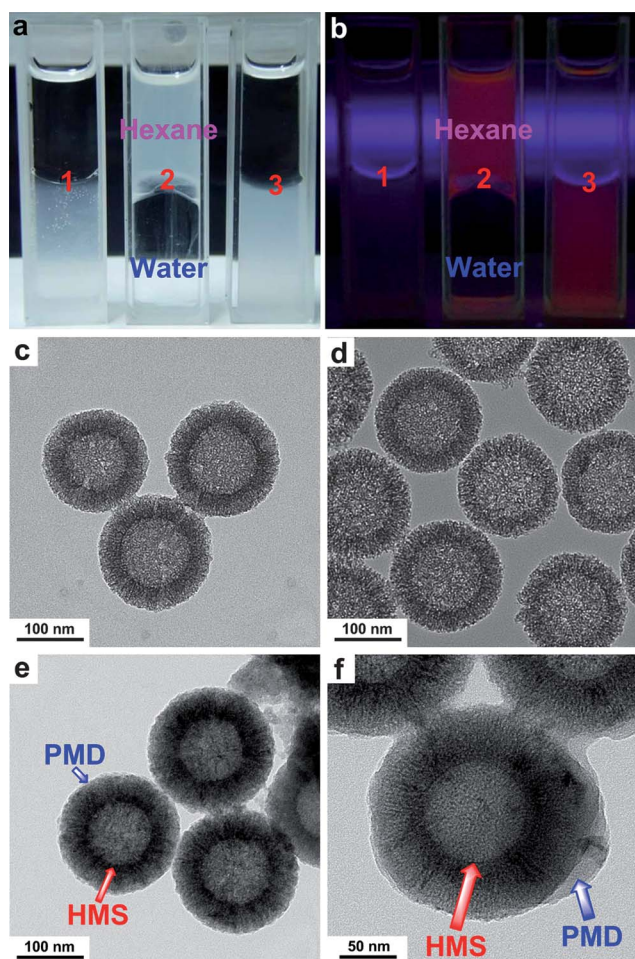


Fig. 3 Photographs of HMS (1), IBU@HMS@YVO₄:Eu³⁺@C18 (2) and IBU@HMS@YVO₄:Eu³⁺@C18@PMD (3) under visible light (a) and UV light ($\lambda = 265$ nm) (b), respectively. TEM images of HMS (c), IBU@HMS@YVO₄:Eu³⁺@C18 (d) and IBU@HMS@YVO₄:Eu³⁺@C18@PMD (e, f).

pure HMS (Fig. 3c) and IBU@HMS@YVO₄:Eu³⁺@C18 (Fig. 3d). TEM images are utilized to observe the microstructure of the particles. Almost no changes were observed between pure HMS and IBU@HMS@YVO₄:Eu³⁺@C18, and both of them maintained good monodispersity with an average diameter of 180 nm and a very clear profile. In contrast, the profile of IBU@HMS@YVO₄:Eu³⁺@C18@PMD became blurred and a thin layer of polymer film with thickness around 10 nm was clearly observed. The coated polymer film would block the pores of the sphere and hinder the penetration of drugs. Furthermore, the prepared IBU@HMS@YVO₄:Eu³⁺@C18@PMD still retains good monodispersity and nanosize, which is very important for application in drug delivery. DLS results (Fig. S2-d, ESI[†]) show that the HMS@YVO₄:Eu³⁺@C18@PMD have an average diameter of 200 nm, with a narrow size distribution (PDI = 0.03), which are consistent with the TEM results.

Properties of IBU@HMS@YVO₄:Eu³⁺@C18@PMD

Determination of drug loading content. Fig. 4 shows the UV absorbance spectra in 60 mg mL⁻¹ IBU hexane solution before and after being loaded by HMS@YVO₄:Eu³⁺@C18. The visible

reduction of UV absorbance between the IBU solution before and after adsorption reflects the reduction of drug concentration, which means drug was loaded into HMS@YVO₄:Eu³⁺@C18; up to 834 mg/g (drug/carrier) of the drug loading content was calculated according to the Beer–Lambert law mentioned above. Such a high drug loading content may be mainly attributed to the hollow core which can store more drug molecules than normal silica nanoparticles.²³ Besides, the modification of the long alkyl chains changed the surface of HMS into hydrophobic, increasing the interaction between surface and drug molecules, making the drug more easily loaded into HMS.⁴¹

Drug release behavior. To study the drug release behavior of the prepared nanoparticles, we first compared the drug release rate of pure HMS and HMS@YVO₄:Eu³⁺@C18 in SBF at 37 °C (Fig. 5). It can be seen that within 10 h, about 70% of IBU can be quickly released from pure HMS, but only about 20% of IBU was released from HMS@YVO₄:Eu³⁺@C18. Even 45 h later, only 40% of IBU was released from HMS@YVO₄:Eu³⁺@C18. The relatively quick drug release of pure HMS may be because that the release media would easily penetrate into the core of pure HMS and the interaction between the Si–OH and carboxyl groups of IBU is weak, so the drug would easily diffuse from the system along release media filled pore channels. However, for the sample modified by long alkyl chains, the wettability of system would be reduced, and the penetration of release media would be more difficult. Besides, the hydrophobic interaction between drug molecules and long alkyl chains would further delay the drug release. Therefore, a long-term drug release system can be achieved by modifying alkyl chains on surface of HMS. Since the anti-cancer drugs can not kill all of cancer cells in a short time and any remaining cancer cells will regrow the tumor, this system can improve the ratio of drug utilization and achieve sustained treatment.

To further investigate pH-stimulated drug release properties of IBU@HMS@YVO₄:Eu³⁺@C18@PMD, the prepared nanoparticles were immersed in SBF at two different pH values (pH 7.4 and 5.0) at 37 °C (Fig. 6). With coating of the functional polymer, the IBU would be blocked in the core of the nanoparticles, and less than 5% leaked out the carrier at pH 7.4 even

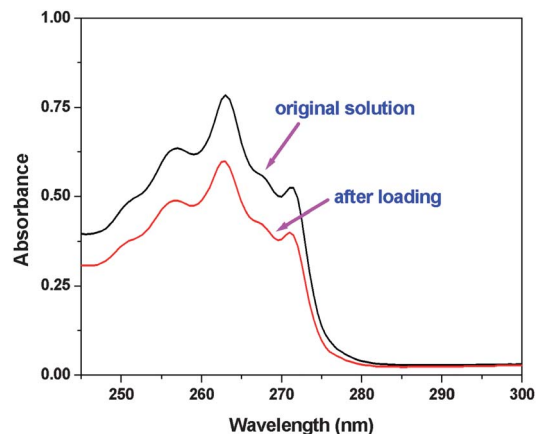


Fig. 4 UV-Vis absorption of ibuprofen solution before and after being loaded by HMS@YVO₄:Eu³⁺@C18.

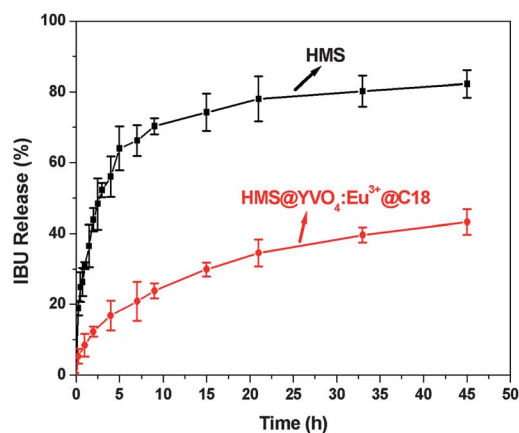


Fig. 5 Release of IBU *in vitro* from drug-loaded HMS and HMS@YVO₄:Eu³⁺@C18 at 37 °C.

after 150 h. When adjusting the pH value to 5.0, the acetal groups of PMD would hydrolyse into hydroxyl groups and the hydrophobic segments would change into hydrophilic segments (H NMR of the hydrolyzed polymer and hydrolysis degree curve are shown in Fig. S6 and Fig. S7, respectively, see ESI[†]), so the polymer will no longer block the pore channels and the drug would be released. However, given the hydrophobic interaction between drug molecules and the long alkyl chains, the drug release is slow and about 80% drug release occurs over 150 h. Hence, a pH-stimulated response and long-term release drug delivery system was prepared successfully.

Cell imaging properties. The cytotoxicity of HMS@YVO₄:Eu³⁺@C18@PMD was assessed at different concentrations by SRB assay with human mouth epidermal carcinoma (KB) cells used as model cells. As shown in Fig. 7a, no cytotoxicity was evident in the preliminary observations of the cells that were treated by HMS@YVO₄:Eu³⁺@C18@PMD for 24 h, and even at as high as 100 μg mL⁻¹ concentration of the carrier, the cell viability was still maintained at more than 80%.

The PL properties of HMS@YVO₄:Eu³⁺@C18@PMD were characterized by excitation and emission spectra, as shown in

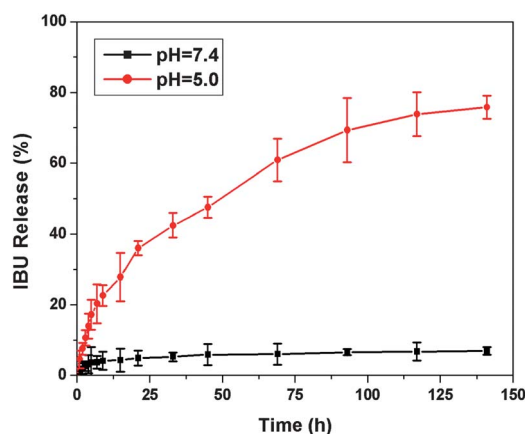


Fig. 6 Release of IBU *in vitro* from drug-loaded HMS@YVO₄:Eu³⁺@C18@PMD at different pH at 37 °C.

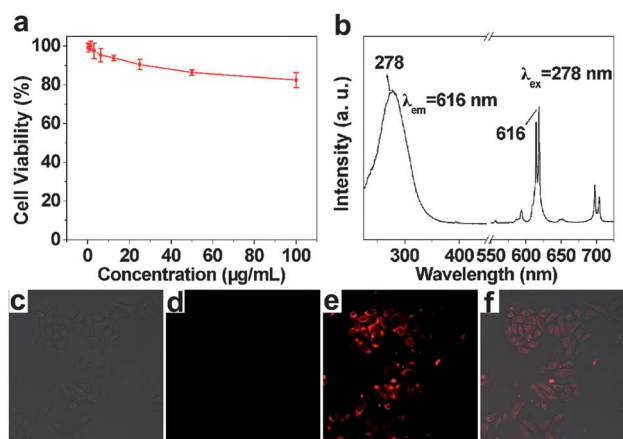


Fig. 7 *In vitro* cell viabilities, measured by SRB assay, after culture of human mouth epidermal carcinoma (KB) cells with HMS@YVO₄:Eu³⁺@C18@PMD as function of concentration and time: (a) excitation (left) and emission (right) spectra of HMS@YVO₄:Eu³⁺@C18@PMD (b); confocal fluorescence microscopy images of KB cells in bright field (c), and exposed to HMS@YVO₄:Eu³⁺@C18@PMD (50 μg mL⁻¹) for 5 min (d), 60 min (e and f).

Fig. 7b, with excitation wavelength of 278 nm and emission wavelength of 616 nm.⁴⁶ Human mouth epidermal carcinoma (KB) cells were exposed to HMS@YVO₄:Eu³⁺@C18@PMD (50 μg mL⁻¹) for 5 and 60 min, respectively. After 5 min of exposure, pale red signals were observed in the cytoplasm, revealed that the samples were entering the KB cells. At an exposure time of up to 60 min (Fig. 7e and f), the fluorescence of cells became stronger, and the profile of cells was clearly visible. Clearly HMS@YVO₄:Eu³⁺@C18@PMD with low cytotoxicity and red fluorescence can enter the cancer cells quickly, which is suitable for cell imaging.

Conclusions

In summary, a facile method for coating HMS with functional polymer through hydrophobic van der Waals interactions has been established. The prepared material IBU@HMS@YVO₄:Eu³⁺@C18@PMD *via* this method has a high drug loading content and can achieve long-term drug release. Besides, this multifunctional material was verified to be a pH stimuli-responsive controlled-release system through designing the structure of the coated polymer and a cell imaging system through modification with a fluorescent material. Clearly, different polymers with other characteristics such as temperature-, light- and enzyme-responsive properties could be easily coated on the surface of silica nanoparticles to satisfy specific requirements of drug delivery.

Acknowledgements

This work was supported by the National Natural Science Foundation of China (Grant Nos. 20876101, 20902065, 21071105 and 21076134), the Natural Science Foundation of the Jiangsu Higher Education Institutions of China (Grant No.09KJB430010) and Innovative Research Team of Advanced Chemical and Biological Materials, Soochow University.

Notes and references

- 1 C. H. Lee, S. H. Cheng, I. P. Huang, J. S. Souris, C. S. Yang, C. Y. Mou and L. W. Lo, *Angew. Chem., Int. Ed.*, 2010, **49**, 8214.
- 2 M. Oishi, H. Hayashi, M. Iijimad and Y. Nagasaki, *J. Mater. Chem.*, 2007, **17**, 3720.
- 3 A. Barnadas, *Cancer Treat. Rev.*, 2005, **31**, S11.
- 4 W. Chen, F. H. Meng, F. Li, S. J. Ji and Z. Y. Zhong, *Biomacromolecules*, 2009, **10**, 1727.
- 5 X. Q. Zhang, R. Lam, X. Y. Xu, E. K. Chow, H. J. Kim and D. Ho, *Adv. Mater.*, 2011, **23**, 4770.
- 6 J. L. Vivero-Escoto, I. I. Slowing, C. W. Wu and V. S.-Y. Lin, *J. Am. Chem. Soc.*, 2009, **131**, 3462.
- 7 S. Angelos, N. M. Khashab, Y. W. Yang, A. Trabolsi, H. A. Khatib, J. F. Stoddart and J. I. Zink, *J. Am. Chem. Soc.*, 2009, **131**, 12912.
- 8 F. H. Chen, Q. Gao and J. Z. Ni, *Nanotechnology*, 2008, **19**, 165103.
- 9 L. Li, K. M. Huh, Y. K. Leeb and S. Y. Kim, *J. Mater. Chem.*, 2011, **21**, 15288.
- 10 J. S. Lu, N. J. Li, Q. F. Xu, J. F. Ge, J. M. Lu and X. W. Xia, *Polymer*, 2010, **51**, 1709.
- 11 L. Sun, W. Liu and C. M. Dong, *Chem. Commun.*, 2011, **47**, 11282.
- 12 M. Hamoudeh, M. A. Kamleh, R. Diab and H. Fessi, *Adv. Drug Delivery Rev.*, 2008, **60**, 1329.
- 13 N. A. Stasko, C. B. Johnson, M. H. Schoenfish, T. A. Johnson and E. L. Holmuhamedov, *Biomacromolecules*, 2007, **8**, 3853.
- 14 E. R. Gillies, T. B. Jonsson and J. M. J. Fréchet, *J. Am. Chem. Soc.*, 2004, **126**, 11936.
- 15 S. Jiang, Y. Zhang, K. M. Lim, E. K. W. Sim and L. Ye, *Nanotechnology*, 2009, **20**, 155101.
- 16 C. T. Kresge, M. E. Leonowicz, W. J. Roth, J. C. Vartuli and J. S. Beck, *Nature*, 1992, **359**, 710.
- 17 M. Vallet-Regí, F. balas and D. Arcos, *Angew. Chem., Int. Ed.*, 2007, **46**, 7548.
- 18 D. Zhao, J. Feng, Q. Huo, N. Melosh, G. H. Fredrickson, B. F. Chmelka and G. D. Stucky, *Science*, 1998, **279**, 548.
- 19 A. L. Doadrio, E. M. B. Sousa, J. C. Doadrio, J. Perez-Pariente, I. Izquierdo-Barba and M. Vallet-Regí, *J. Controlled Release*, 2004, **97**, 125.
- 20 A. Schlossbauer, J. Kecht and T. Bein, *Angew. Chem., Int. Ed.*, 2009, **48**, 3092.
- 21 L. Du, S. Liao, H. A. Khatib, J. F. Stoddart and J. I. Zink, *J. Am. Chem. Soc.*, 2009, **131**, 15136.
- 22 Y. F. Zhu, J. L. Shi, W. H. Shen, X. P. Dong, J. W. Feng, M. L. Ruan and Y. S. Li, *Angew. Chem., Int. Ed.*, 2005, **44**, 5083.
- 23 W. R. Zhao, M. D. Lang, Y. S. Li, L. Li and J. L. Shi, *J. Mater. Chem.*, 2009, **19**, 2778.
- 24 W. R. Zhao, J. L. Gu, L. X. Zhang, H. R. Chen and J. L. Shi, *J. Am. Chem. Soc.*, 2005, **127**, 8916.
- 25 W. R. Zhao, H. R. Chen, Y. S. Li, L. Li, M. D. Lang and J. L. Shi, *Adv. Funct. Mater.*, 2008, **18**, 2780.
- 26 Y. Chen, H. R. Chen, L. M. Guo, Q. J. He, F. Chen, J. Zhou, J. W. Feng and Jianlin Shi, *ACS Nano*, 2010, **4**, 529.
- 27 J. Lu, M. Liong, Z. X. Li, J. I. Zink and F. Tamanoi, *Small*, 2010, **6**, 1794.
- 28 E. Aznar, M. D. Marcos, R. ezMartínez-Mán, F. Sancenon, J. Soto, P. Amoros and C. Guillem, *J. Am. Chem. Soc.*, 2009, **131**, 6833.
- 29 C. Y. Lai, B. G. Trewyn, D. M. Jeftinija, K. Jeftinija, S. Xu, S. Jeftinija and V. S. Y. Lin, *J. Am. Chem. Soc.*, 2003, **125**, 4451.
- 30 R. Liu, Y. Zhang, X. Zhao, A. Agarwal, L. J. Mueller and P. Y. Feng, *J. Am. Chem. Soc.*, 2010, **132**, 1500.
- 31 K. Patel, S. Angelos, W. R. Dichtel, A. Coskun, Y. W. Yang, J. I. Zink and J. F. Stoddart, *J. Am. Chem. Soc.*, 2008, **130**, 2382.
- 32 Y. L. Choi, J. Jaworski, M. L. Seo, S. J. Lee and J. H. Jung, *J. Mater. Chem.*, 2011, **21**, 7882.
- 33 C. Chen, J. Geng, F. Pu, X. Yang, J. Ren and X. Qu, *Angew. Chem.*, 2011, **123**, 912.
- 34 C. Coll, L. Mondragon, R. Martínez-Máñez, F. Sancenon, M. D. Marcos, J. Soto, P. Amoros and E. Pérez-Payá, *Angew. Chem., Int. Ed.*, 2011, **50**, 2138.
- 35 E. Climent, R. Martínez-Máñez, F. Sancenon, M. D. Marcos, J. Soto, A. Maquieira and P. Amoros, *Angew. Chem., Int. Ed.*, 2010, **49**, 7281.
- 36 Q. Gao, Y. Xu, D. Wu, Y. Sun and X. Li, *J. Phys. Chem. C*, 2009, **113**, 12753.
- 37 H. Zou, S. Wu and J. Shen, *Chem. Rev.*, 2008, **108**, 3893.
- 38 M. barari and N. Sharifi-Sanjanai, *J. Appl. Polym. Sci.*, 2008, **110**, 929.
- 39 P. W. Chung, R. Kumar, M. Pruski and V. S.-Y. Lin, *Adv. Funct. Mater.*, 2008, **18**, 1390.
- 40 A. Papat, S. B. Hartono, F. Stahr, J. Liu, S. Z. Qiao and G. Q. (Max) Lu, *Nanoscale*, 2011, **3**, 2801.
- 41 J. C. Doadrio, E. M. B. Sousa, I. Izquierdo-Barba, A. L. Doadrio, J. Perez-Pariente and M. Vallet-Regí, *J. Mater. Chem.*, 2006, **16**, 462.
- 42 E. Aznar, L. Mondragon, J. Ros-Lis, F. Sancenon, M. D. Marcos, R. Martínez-Máñez, J. Soto, E. Pérez-Payá and P. Amoros, *Angew. Chem., Int. Ed.*, 2011, **50**, 11172.
- 43 D. Y. Chen, N. J. Li, H. W., X. W. Xia, Q. F. Xu, J. F. Ge, J. M. Lu and Y. G. Li, *Chem. Commun.*, 2010, **46**, 6708.
- 44 F. Wang, W. B. Tan, Y. Zhang, X. Fan and M. Wang, *Nanotechnology*, 2006, **17**, R1.
- 45 V. Buissette, D. Giaume, T. Gacoin and J. P. Boilot, *J. Mater. Chem.*, 2006, **16**, 529.
- 46 P. P. Yang, Z. W. Quan, Z. Y. Hou, C. X. Li, X. J. Kang, Z. Y. Cheng and J. Lin, *Biomaterials*, 2009, **30**, 4786.
- 47 G. Qi, Y. B. Wang, L. Estevez, A. K. Switzer, X. N. Duan, X. F. Yang and E. P. Giannelis, *Chem. Mater.*, 2010, **22**, 2693.
- 48 C. Yan, J. K. Kepa, D. Siegel, I. J. Stratford and D. Ross, *Mol. Pharmacol.*, 2008, **74**, 1657.